Mean-field theory of the Ising random-anisotropy-axis model in the large-component limit

D. R. C. Dominguez and W. K. Theumann
Instituto de Física, Universidade Federal do Rio Grande do Sul,
Caixa Postal 15051, 91501-970, Porto Alegre, RS, Brazil
(Received 1 February 1993; revised manuscript received 22 April 1993)

The Ising random-anisotropy-axis model with additional noncubic anisotropy is investigated in mean-field theory in the limit $p \to \infty$ for p-component random vectors on a lattice of N sites. The effects of anisotropy for statistically independent and identically distributed random-vector components with a trimodal probability distribution are studied in the limits $\alpha \equiv p/N = 0$ and $\alpha > 0$. Ferromagnetic, mixed, and residual ordered phases are found in the first case, while only mixed ordered and spin-glass phases are found for the latter. Phase diagrams with explicit phase boundaries are obtained.

I. INTRODUCTION

The random-anisotropy-axis model (RAM), introduced by Harris, Plischke, and Zuckermann[1] to describe the unusual properties of amorphous intermetallic compounds, such as $TbFe_2$, is defined by the Hamiltonian

$$H = -\sum_{\langle i,j \rangle} J_{ij}\, \mathbf{s}_i \cdot \mathbf{s}_j - D \sum_i (\mathbf{n}_i \cdot \mathbf{s}_i)^2 - \mathbf{h} \cdot \sum_i \mathbf{s}_i \quad (1)$$

for p-component classical unit "spins" $\mathbf{s}_i$, with nearest-neighbor ferromagnetic exchange interactions J_{ij} on the sites $i = 1, \ldots, N$ of a d-dimensional lattice. Here, $\mathbf{n}_i$ are unit vectors that are randomly oriented from site to site, and the anisotropy strength D is assumed to be the same at all sites, while $\mathbf{h}$ is a uniform, nonrandom, external field.

There has been great interest in the model due to the competition between long-range magnetic order and the global disorder built into the random anisotropy. It has also been viewed as an alternative[2] to the Edwards-Anderson (EA) model for a spin glass.[3] Although the model explains some of the extensive experimental results on amorphous alloys that are now available,[4] the nature of the ordered "ferromagnetic" and "spin-glass" phases, and when they should be expected to appear, is still a matter of some controversy.[5–14]

The strong-anisotropy limit $D/J \to \infty$ has been studied numerically[15] and in mean-field theory (MFT),[16] the latter by Fischer and Zippelius[17] (FZ), and by other means.[10–14] In this limit each spin is aligned along its local anisotropy axis, $\mathbf{s}_i = \mathbf{n}_i \sigma_i$, in which $\sigma_i = \pm 1$. The Hamiltonian then becomes, apart from a constant,

$$H_I = -\sum_{(i,j)} J_{ij}^I \sigma_i \sigma_j - \sum_i h_i \sigma_i, \quad (2)$$

which is that of a particular random-bond Ising model, the so-called Ising random-anisotropy-axis model (IRAM), where

$$J_{ij}^I = J_{ij}\, \mathbf{n}_i \cdot \mathbf{n}_j, \qquad h_i = \mathbf{h} \cdot \mathbf{n}_i, \quad (3)$$

in which the $\mathbf{n}_i$ are constrained unit vectors. Although in pratice the average over random angles that appears in calculating the thermodynamic properties of the model is sometimes replaced[6,7] by an average over an effective distribution of independent random bonds, it has been pointed out recently that this is not correct, in general, except in the limit $p \to \infty$.[11] In this case, the problem is uninteresting since the model reduces to the already explored EA model, *unless* the distribution of $\mathbf{n}_i$ is neither isotropic nor a Gaussian.

In the large-p limit, the model becomes identical to the Hopfield model for neural networks[18–20] if the n_i^μ are discrete independent random variables that take the values ± 1, and this model is known to have a different behavior from the EA model even in the limit $p \to \infty$.[19–21]

The relevance of the probability distribution of $\mathbf{n}_i$ for the RAM has been pointed out by Harris, Plischke, and Zuckermann[1]. In the case of the IRAM, the magnetization states are degenerate for an isotropic distribution of $\mathbf{n}_i$, due to the underlying $O(p)$ symmetry of the model. FZ showed, in MFT for finite p, that a random hypercubic anisotropy stabilizes a ferromagnetic state in the IRAM with a symmetric diagonal magnetization that has equal components along any of the hypercubic axes.

The purpose of the present paper is to study further the role of the distribution functions for n_i^μ in the IRAM, with particular emphasis on the behavior when $p \to \infty$ while $\alpha = p/N$ remains finite, the so-called α limit.[22] The related Hopfield model of neural networks is known to have a spin-glass state for α larger than a critical value and local or globally stable one-component ferromagnetic (Mattis) states below this value.[19] These states arise as a "condensation" of a single component of the magnetization becoming of $O(1)$, while the remaining $(p-1)$ components are of $O(1\sqrt{N})$.

The behavior of the IRAM as a function of $\tilde{\alpha} \equiv p/z$, where z is the coordination number of the lattice, has been studied on a Cayley tree[10] and on hypercubical lattices[11] for *finite* p and z. These works also suggest a spin-glass or ferromagnetic behavior for $\tilde{\alpha}$ above or below a critical value, respectively.

The outline of the paper is the following. In Sec. II we state the model and introduce the relevant order parameters and probability distributions for n_i^μ. The replacement of the uniform distribution appropriate for the "hard" constraint by an often-used Gaussian is also discussed there. In Sec. III we deal with the large-p behavior when $\alpha = 0$, and in Sec. IV we consider the finite-α case. We end with a critical discussion in Sec. V.

II. THE MODEL

The Hamiltonian of the IRAM with infinite-range interactions, suitable for MFT, is given by

$$H_I = -\frac{J}{2N}\sum_{i,j}\sum_{\mu=1}^{p} n_i^\mu n_j^\mu \sigma_i \sigma_j - \sum_i \sigma_i \sum_\mu h_\mu n_i^\mu, \quad (4)$$

where the n_i^μ, for $\mu = 1, ..., p$, will be taken as identically distributed independent variables.

The magnetic variable of interest for the IRAM is defined here as

$$\mathbf{m}_N = \frac{1}{N}\sum_i \mathbf{n}_i \sigma_i. \quad (5)$$

The thermal average with the Boltzmann factor $\exp(-\beta H_I)$, which will be denoted by angular brackets, and the self-averaging property for finite p yield the magnetic order parameter

$$\mathbf{m} = \lim_{N\to\infty} \langle \mathbf{m}_N \rangle = [\mathbf{n}\langle\sigma\rangle]_n, \quad (6)$$

where the square brackets denote the configurational average over the probability distribution of n_i^μ. Thus, $\mathbf{m}$ is the analog of the overlap vector in neural networks. The right-hand side of Eq. (6) will still be used to define the magnetic order parameter for all p, even in the α limit, in which case self-averaging no longer applies. The spin-glass order parameter used here is the usual replica symmetric $q = q_{\alpha\beta}$,[3,23]

$$q_{\alpha\beta} = [\langle \mathbf{s}^\alpha \rangle \cdot \langle \mathbf{s}^\beta \rangle]_n = [\langle \sigma^\alpha \rangle \langle \sigma^\beta \rangle]_n, \quad \alpha \neq \beta, \quad (7)$$

in the replica space α, β necessary to perform the configurational average for the α limit.

A. Probability distributions

An isotropic probability distribution has already been used by Harris, Plischke, and Zuckermann[1]. The anisotropic distribution

$$p(\mathbf{n}_i) = \frac{1-r}{\Omega_p} + \frac{r}{2p}\sum_{s=1}^{p}[\delta(\mathbf{n}_i - \mathbf{e}_s) + \delta(\mathbf{n}_i + \mathbf{e}_s)], \quad (8)$$

with constrained random axis, has been used in the IRAM by FZ. The first term is isotropic with the vector $\mathbf{n}_i$ on the unit sphere of area $\Omega_p = 2\pi^{-p/2}/\Gamma(p/2)$, in p-dimensional space, $r(0 < r < 1)$ is the anisotropy strength, and $\mathbf{e}_s$ is a unit vector in the direction of a crystal axis. The δ functions are Kronecker deltas, equal to 1 if $\mathbf{n}_i = \pm\mathbf{e}_s$ and 0 otherwise, implying that $n_i^\mu = \pm 1$, with equal probabilities, for one component of $\mathbf{n}_i$ at a time and zero for the remaining $(p-1)$ components.

We consider two distributions of statistically independent random variables in this work. One is the sometimes employed Gaussian distribution for statistically independent and identically distributed components n_i^μ of mean zero and unit variance,[6,7]

$$d\Phi(\vec{n}_i) = d\mathbf{n}_i\ \phi(\mathbf{n}_i) = \prod_{\mu=1}^{p}[dn_i^\mu\ \phi(n_i^\mu)], \quad (9)$$

used here only for comparison, in which

$$\phi(x) = \frac{1}{\sqrt{2\pi}} e^{-x^2/2}. \quad (10)$$

In this way, the random-axis vector also acquires a varying modulus. Nevertheless, the Ising random-axis limit $D/J \to \infty$ is still meaningful in the large-p limit, in that $(D/J)|\mathbf{n}_i|^2$ does not become of order 1 or smaller on a sizable set of lattice sites, since $\gamma \equiv \mathbf{n}^2 = p$ for almost every site i in this limit, with relative dispersion $\sigma(\gamma)/[\gamma]_n = O(1/\sqrt{p})$.

The other case we consider is a variant of (8), given by the trimodal distribution

$$dP(\mathbf{n}_i) = \prod_{\mu=1}^{p}[dn_i^\mu\ p(n_i^\mu)] \quad (11)$$

of statistically independent and identically distributed components $x \equiv n_i^\mu$, in which

$$p(x) = \frac{b}{2}\{\delta(x-a) + \delta(x+a)\} + u\delta(x), \qquad u \equiv 1 - b, \quad (12)$$

where b is a real constant such that $0 < b \leq 1$ and $a = 1/\sqrt{b}$ (there is no loss of generality with this choice). Since $[n_\mu^4]_n = 1/b$, a finite lower limit to b is necessary in order to still have a vanishing relative fluctuation of $\mathbf{n}_i^2$ for a meaningful large-D limit, as pointed out above. When b=1 the distribution reduces to that for the Hopfield model. In general, a typical term in the product in Eq. (11) involves a sum of terms $\delta(\mathbf{n} \pm \mathbf{a}_s)$ on each site over all the permutations of $s \leq p$ nonzero components in a vector $\mathbf{a}_s$.

III. LARGE-p BEHAVIOR WITH $\alpha = 0$

The Hamiltonian, Eq. (4), may be written as

$$H_I = -\frac{J}{2} N \mathbf{m}_N^2 - N\mathbf{h} \cdot \mathbf{m}_N, \tag{13}$$

making use of Eq. (5). We consider first the large-p limit when $\alpha = 0$, so that the now standard procedure for the Hopfield model of neural networks for finite p can be used to find the free energy per site of the IRAM in MF theory as[19,20]

$$f = \frac{J}{2}\mathbf{m}^2 - T[\ln\left(2\cosh\{\beta(J\mathbf{m} + \mathbf{h}) \cdot \mathbf{n}\}\right)]_n. \tag{14}$$

Here, $T = \beta^{-1}$ is the temperature in units of energy and the magnetic order parameter $\mathbf{m} = (m_1, ..., m_p)$ is given by the solution of the equation

$$\mathbf{m} = [\mathbf{n} \tanh\{\beta(J\mathbf{m} + \mathbf{h}) \cdot \mathbf{n}\}]_n, \tag{15}$$

with components satisfying $m_\mu = -\partial f / \partial h_\mu$.

It is appropriate to recall here that the solutions in zero field for finite p are degenerate for an isotropic distribution of n_i^μ [Eq. (8) with $r = 0$] due to the invariance under a uniform rotation in p-component space and that the degeneracy is lifted for $r \neq 0$. In this case the only solutions are the s-component symmetric, $\mathbf{m} = m_s(1, ..., 1, 0, ..., 0)$, whose free energy is given, near the critical temperature $T_c = 1$ and at $T = 0$, by

$$f_s^c = -\frac{\tau^2}{4}\frac{s}{p}\left[(1-r)\frac{s}{p} + \frac{r}{3}\right]^{-1},$$
$$f_s^0 = -\{(1-r)\sqrt{2/\pi} + r\sqrt{s/p}\}^2/2, \tag{16}$$

respectively, in the large-p limit,where

$$\tau \equiv 1 - T. \tag{17}$$

Thus the symmetric state with the maximum number of nonzero components, in which $s = p$, has the lowest free energy.[17] The problem with rotationally invariant distributions is that the degenerate solutions are only marginally stable.[20]

A number of interesting situations arise with the new probability distributions, Eq. (12), in the large-p limit. In this case there can be only a finite number of nonvanishing components of the magnetization. Assuming that there is only one of them, say, $m = m_1$, and that there are $p-1$ residual components of $O(1/\sqrt{p})$, one may write, in the case of a statistically independent distribution of random-axis components,

$$\mathbf{m} \cdot \mathbf{n} = m\rho + Rz, \tag{18}$$

dropping the index in m, where ρ is a single component of $\mathbf{n}$, while $Rz = \sum_{\mu>1} m_\mu n^\mu$ is the sum of the $(p-1)$ remaining terms. Since each term is independent, this sum is distributed according to a Gaussian, with mean zero and variance $R^2 = \sum_{\mu>1} m_\mu^2$. Thus z is also Gaussian with mean zero and unit variance.

The components of the magnetization in zero field are then given by

$$m = [\rho \tanh\{\beta(m\rho + Rz)\}]_{\rho,z} \tag{19}$$

and

$$R = [z \tanh\{\beta(m\rho + Rz)\}]_{\rho,z}, \tag{20}$$

taking, for simplicity, $J = 1$, where the averages of the quantities in square brackets are over the distributions of ρ and z.

If ρ is distributed according to Eq. (12), in addition to the paramagnetic high-temperature phase, where $m = 0$ and $R = 0$, there could be three further phases characterized as

$$F : \binom{m\neq 0}{R=0}, \quad M : \binom{m\neq 0}{R\neq 0}, \quad R : \binom{m=0}{R\neq 0}, \tag{21}$$

which are the ferromagnetic (Mattis), mixed, and residual ordered states, respectively. Depending on the value of b, one or the other states may be stable. The first two (F and M) are genuinely ordered states, with a finite magnetization, while the last one is a state with, at most, local order, signaled by a nonvanishing EA order parameter

$$q = [\tanh^2(\beta R z)]_z, \tag{22}$$

which follows from Eq. (20) through an integration by parts. Note that $q \to 1$, while $m = 0$ as $T \to 0$.

Solving Eqs. (19) and (20) for $R \ll 1$ yields the phase boundary

$$l = \tanh(\beta l) \tag{23}$$

of continuous transitions in R, shown in Fig. 1, between the F and M phases, in which $l = m/\sqrt{b}$. We also find the finite magnetization

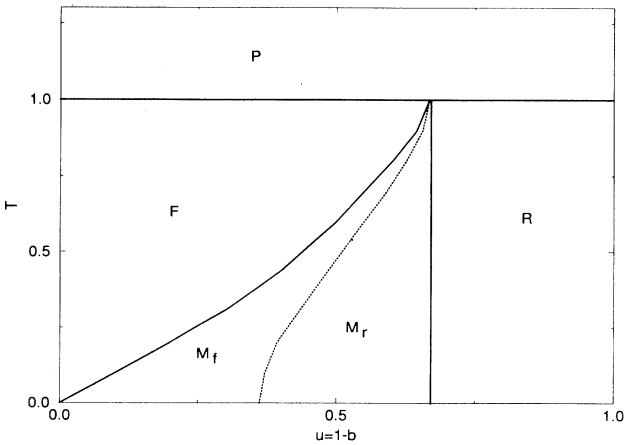

FIG. 1. Phase diagram for $\alpha = 0$, indicating the paramagnetic (P), ferromagnetic (F), mixed (M), and residual (R) phases defined in Eq. (21). In the region M_f of the mixed phase the free energy of the ferromagnetic state is the next-to-lowest one, while in the region M_r the residual state has the next-to-lowest free energy.

$$m = \sqrt{\tau} \tag{24}$$

along this boundary, in extension to the familiar behavior of the neural-network problem. Note, however, that here in the random-axis model, there is a whole region of ferromagnetic states in the (u,T) plane enclosed by the phase boundary.

On the other hand, solving Eqs. (19) and (20) for $m \ll 1$ yields the boundary

$$b = 1/3 \quad \text{for all} \quad T \leq 1, \tag{25}$$

also shown in Fig. 1, between the M and R phases, together with the order parameter

$$q = \tau \tag{26}$$

along that boundary.

The stability of the various phases has been studied by means of two criteria. First, the states of lowest free energy have been selected as the stable phases, and second, these have been checked against a local stability criterion that involves the eigenvalues of the second-derivative matrix of the free energy, Eq. (14). Both criteria complement each other. If the free energy for two different solutions for the order parameters is truly convex (all eigenvalues being positive), then, as usual, the lower free energy yields the stable phase. The same applies if one of the solutions is not truly convex (for instance, "flat" or concave in at least one direction), as long as it is not the lowest free energy. If, instead, the lowest free energy is flat in at least one direction, as would be the case with one eigenvalue being zero, there cannot be a truly stable state.

Calling f_F, f_M, and f_R the free energies per spin in each of the states defined in Eq. (21), it turns out that $f_F < f_R$ in the F phase and $f_M < \{f_F, f_R\}$ in the M phase, f_F being less than f_R in region M_f in Fig. 1, while $f_F > f_R$ in region M_r and $f_R < f_M$ in the R phase. The state M does not exist either in the F or in the R phases.

On the other hand, considering the second-derivative matrix of the free energy, with elements

$$D_m \equiv \frac{\partial^2 f}{\partial m^2} = 1 - \beta\big(1 - [\rho^2 \tanh^2(\beta A)]_{\rho,z}\big), \tag{27}$$

$$D_R \equiv \frac{\partial^2 f}{\partial R^2} = 1 - \beta\big(1 - [z^2 \tanh^2(\beta A)]_{\rho,z}\big), \tag{28}$$

$$Q \equiv \frac{\partial^2 f}{\partial m \partial R} = \beta[\rho z \tanh^2(\beta A)]_{\rho,z}, \tag{29}$$

in which $A \equiv m\rho + Rz$, the smallest eigenvalue

$$\lambda = (D_m + D_R)/2 - \sqrt{(D_m - D_R)^2/4 - (\beta Q)^2} \tag{30}$$

becomes $\lambda = \min(D_m, D_R)$, when $Q = 0$. This is the case if either m or R are zero. Looking at this lowest eingenvalue in each of the three states, $\lambda^F, \lambda^M, \lambda^R$, we find that $\lambda^F \geq 0$, in the F phase. The equality holds in the F-M phase boundary, Eq. (23). On the other hand, λ^F becomes negative to the right of this boundary, where the M state is stable within the region M_f and M_r indicated in Fig. 1, with $\lambda^M > 0$.

At the other extreme, in the R phase, we have $\lambda^R = 0$, while $\lambda^F < 0$. The former is an eigenvalue corresponding to a marginal mode, meaning either a local flatness of the free energy or a region turning into an unstable state. It should be noted that the solution with $m = 0$ and $R \neq 0$ is marginally stable also in the other phases below T_c. We take this as a warning that the limit $p \to \infty$ with $\alpha = 0$ is a marginal situation beyond which (i.e., when $\alpha > 0$, no matter how small) a true spin-glass state should appear.

IV. α LIMIT FOR LARGE-p BEHAVIOR

The analogy with the neural-network problem suggests that a number of interesting features should appear in the random-axis model in the α limit. To deal with this case one has to resort to the replica method, as in the neural-network problem.[21]

The free energy per spin is then given by

$$f = -\lim_{\nu \to 0} \lim_{N \to \infty} \frac{[Z^\nu]_n - 1}{\nu N \beta}, \tag{31}$$

where the configurational average is taken over the ν-fold replicated partition function

$$Z^\nu = Tr_\sigma \, e^{-\beta H_I^\nu}. \tag{32}$$

The ν-replicated Hamiltonian in zero field is here

$$H_I^\nu = -\frac{N}{2} \sum_{\gamma=1}^{\nu} \mathbf{m}_{N\gamma}^2, \tag{33}$$

$$\mathbf{m}_{N\gamma} = \frac{1}{N} \sum_i \mathbf{n}_i \sigma_i^\gamma. \tag{34}$$

The quadratic form in the exponential of Eq. (32) is linearized, as usual, by means of a Gaussian transformation that yields

$$Z^\nu = e^{-\beta p \nu/2} Tr_\sigma \int \prod_\gamma \left\{ \frac{d\mathbf{m}_\gamma}{(2\pi)^{p/2}} \exp\left[-\beta N \left(\frac{\mathbf{m}_\gamma^2}{2} - \frac{\mathbf{m}_\gamma}{N} \cdot \sum_i \mathbf{n}_i \sigma_i^\gamma \right) \right] \right\}. \tag{35}$$

The extremum of a saddle-point integration, in the large-N limit, provides a physical meaning for the $\mathbf{m}_\gamma$ as the magnetic order parameter whose components are

$$m_\gamma^\mu = \frac{1}{N} \left[\sum_i n_i^\mu \langle \sigma_i^\gamma \rangle \right]_n \tag{36}$$

for a given replica γ.

As in the $\alpha = 0$ case, a finite number of m_γ^μ's may condense macroscopically, while an asymptotically large number of residual components may be of $O(1/\sqrt{N})$. In the case of a constrained probability distribution, such as Eq. (8), it is not possible to separate and integrate out

the residual components, as one would like to do, in accordance to standard practice.[21] We consider therefore, in the following, only statistically independent distributions.

For simplicity, we assume first that there is only one component, say, m_1^γ, that condenses macroscopically (we consider the case of more components below) and we recall that the remaining $(p-1)$ components m_μ^γ are microscopic, in order to have a well-defined thermodynamic limit of Eq. (35). We denote the corresponding random-axis vector components by

$$\mathbf{n} = \begin{pmatrix} \rho \\ \boldsymbol{\xi} \end{pmatrix}, \quad \boldsymbol{\xi} = \{n_{\mu>1}\}. \tag{37}$$

The average over $\boldsymbol{\xi}$ can, as usual, be taken out of the trace and written as

$$B_i = [e^{\mathbf{a}_i \cdot \boldsymbol{\xi}_i}]_\xi, \tag{38}$$

in which

$$\mathbf{a}_i = \beta \sum_\gamma \mathbf{m}_\gamma \sigma_i^\gamma. \tag{39}$$

For any distribution of statistically independent ξ_i^μ, in particular for Eq. (12), of mean 0 and variance 1, the central-limit theorem yields, in the limit $p \to \infty$,

$$\prod_i B_i = \exp\left(\sum_i \mathbf{a}_i^2/2\right), \tag{40}$$

in which

$$\sum_i \mathbf{a}_i^2 = \beta N \sum_{\mu>1} \sum_{\gamma\omega} m_\gamma^\mu C_{\gamma\omega} m_\omega^\mu, \tag{41}$$

where

$$C_{\gamma\omega} = \beta \sum_i \sigma_i^\gamma \sigma_i^\omega / N. \tag{42}$$

Using this result in Eq. (35), performing then the integration over $\mathbf{m}_\gamma$, and carrying out the trace over σ before the configurational average over the "low" component ρ, one obtains, for the free energy per spin in the replica symmetric calculation,[21]

$$f = \frac{\alpha}{2} f_C + \frac{m^2}{2} + \frac{CR^2}{2} - T[\ln\left(2\cosh\{\beta(Rz + m\rho)\}\right)]_{\rho,z}, \tag{43}$$

where

$$f_C = 1 + T\ln(1-C) - \frac{q}{1-C}. \tag{44}$$

The magnetic and spin-glass (SG) order parameters that describe the stationary states are, respectively,

$$m \equiv m_\gamma^1 = [\rho\langle\sigma^\gamma\rangle]_{\rho,z}, \quad \text{all } \gamma,$$
$$q \equiv q_{\alpha\beta}, \ \alpha \neq \beta, \tag{45}$$

assuming replica symmetry, while

$$C = \beta(1-q) \tag{46}$$

and

$$R^2 = \left[\sum_{\mu>1} m_\mu^2\right]_z \tag{47}$$

is the variance for the overlap

$$m_\mu \equiv N^{-1} \sum_i \xi_i^\mu \langle\sigma_i\rangle \tag{48}$$

of a configuration of spins with the high ($\mu > 1$) random-axis components. In these expressions, $[\cdots]_z = \int d\Phi(z) \cdots$ denotes the average over the Gaussian noise, in the notation of Eqs. (9) and (10). The parameter R is related to the auxiliary parameter r in Ref. 21 by means of

$$R \equiv \sqrt{\alpha r} = \frac{\sqrt{\alpha q}}{1-C} \tag{49}$$

and accounts for nonmagnetic ordering of the remaining $(p-1)$ components, in that the local magnetic moment may be finite without long-range magnetic ordering, as in a SG phase.

The order parameters satisfy the equations

$$m = [\rho \tanh(\beta A)]_{\rho,z}, \tag{50}$$

$$q = [\tanh^2(\beta A)]_{\rho,z}, \tag{51}$$

where $A = Rz + m\rho$. Transforming Eq. (51) by means of an integration by parts, with Eq. (49), yields

$$R = \sqrt{\alpha q} + [z \tanh(\beta A)]_{\rho,z}, \tag{52}$$

in distinction to the $\alpha = 0$ case, Eq. (20). Note, however, that the latter is recovered if $\alpha = 0$. There is then the possibility of having, again, a ferromagnetic (F) phase, where $m \neq 0$, $R = 0$, a mixed (M) phase in which $m \neq 0$, $R \neq 0$, and there can now be also a spin-glass (SG) phase with $m = 0$, $R \neq 0$, besides a paramagnetic (P) phase where $m = 0 = R$.

It is interesting to consider first the case where ρ is distributed according to the Gaussian in Eq. (10). For the sum in A, the variance becomes $\Delta^2 = R^2 + m^2$ and the solution of Eqs. (49)–(51) yields $C \to 1$, that is, $q \to 1 - T$ and $R \to \infty$. The magnetization is then

$$m = [\rho \operatorname{sgn}(z)]_{\rho,z} = 0 \tag{53}$$

for all finite T, in place of the marginally stable magnetic ordering we had at $\alpha = 0$, for a purely isotropic distribution.

We consider next the trimodal distribution for ρ and deal first with the zero-temperature ($\beta = \infty$) case. The equations for the order parameters become, in this limit,

$$m = \sqrt{b}\,\mathrm{erf}(x), \tag{54}$$

$$R = \sqrt{\alpha} + (1 - b + be^{-x^2/2})\sqrt{\frac{2}{\pi}}, \tag{55}$$

where

$$\mathrm{erf}(x/\sqrt{2}) = 2\int_0^x dz\ \phi(z), \tag{56}$$

$\phi(x)$ being given by Eq. (10), and

$$x \equiv \frac{m}{R\sqrt{b}}. \tag{57}$$

When $b = 1$ there are two solutions: (i) $m \neq 0$, $R \neq 0$, as in the M phase, and (ii) $m = 0$, $R = \sqrt{\alpha} + \sqrt{2/\pi}$, corresponding to a SG phase, with microscopic energy barriers of $O(\alpha^{-1})$. The former is the more stable phase below a critical $\alpha = 0.051$, while the latter appears as a "melting" of vanishingly small symmetric mixture states.[21] Note that $R = 0$ is a solution when $\alpha = 0$, leaving an F phase. In distinction to this, when $b \neq 1$, F never appears, since $R > (1-b)\sqrt{2/\pi}$ for any α.

Combining Eqs. (54) and (55) into the single equation

$$x = \frac{\mathrm{erf}(x/\sqrt{2})}{\sqrt{\alpha} + (u + be^{-x^2/2})\sqrt{\frac{2}{\pi}}}, \tag{58}$$

in which $u = 1 - b$, shows that there is always a SG solution $x = 0 = m$, for any b and any α. This is the only solution above the upper phase boundary shown in the zero-temperature phase diagram of Fig. 2. A finite magnetization m and a nonzero residual R appear as an M state at this first-order phase boundary, when $b \neq 1$, below which there are first locally stable M states until a second, lower boundary is reached where these states become globally stable with a lower energy than the SG states. This behavior is quite different from that in the $b = 1$ limit (the neural-network problem) where locally and globally stable ferromagnetic (F) states appear with decreasing α. Thus, there is a changeover in behavior in the random-axis model when $u = 0$.

The situation in the finite-temperature case ($\beta < \infty$) is

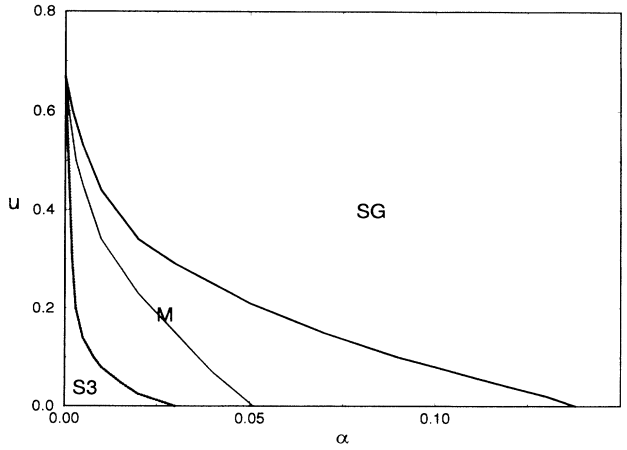

FIG. 2. Zero-temperature diagram for finite α, showing the upper and lower phase boundaries, below which the M state is locally and globally stable, respectively. The dotted line is the boundary for locally stable symmetric solutions with three finite components (cf. Sec. IV). The spin-glass state is the only solution above the upper boundary.

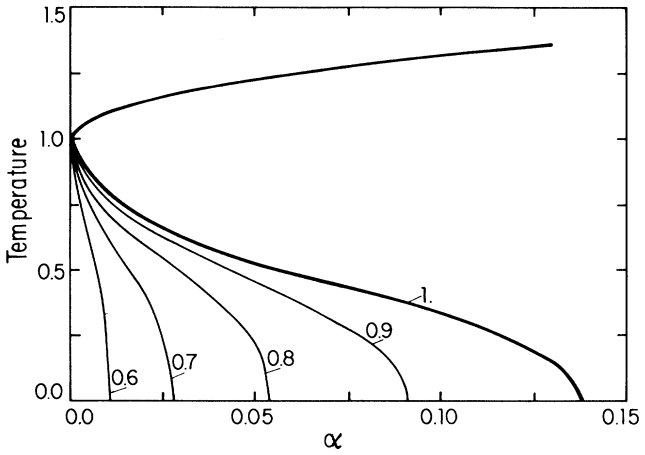

FIG. 3. Phase diagram in the T-α plane for several values of b. The upper curve is the paramagnetic to spin-glass phase boundary, while the lower curves are the phase boundaries for locally stable M states.

shown in the phase diagram exhibited in Fig. 3, where the curves below the upper critical line $T_g = 1+\sqrt{\alpha}$, separating paramagnetic from SG behavior, for all b, represent the transitions from SG to locally stable M-state behavior, for various values of b. Thus, the mixed states remain relevant for finite temperature, except in the limit $\alpha \to 0$. Indeed, only at the $\alpha = 0$ axis may the M states change into F states through the vanishing of R, in accordance with the remark above.

We come back now to the solutions with more than a single component that condense macroscopically. There are, of course, many such solutions, but the relevant question is, what is the fraction of phase space occupied by a given solution? A zero-temperature calculation should give an upper bound, and we consider the symmetric solution with s finite and $(p - s)$ vanishingly small components. The random-axis vector components are then

$$\begin{aligned} \mathbf{n} &= \begin{pmatrix} \boldsymbol{\rho} \\ \boldsymbol{\xi} \end{pmatrix}, \\ \boldsymbol{\rho} &= \{n_{\mu \le s}\}, \\ \boldsymbol{\xi} &= \{n_{\mu > s}\}, \end{aligned} \tag{59}$$

in place of Eq. (37). With the replica-symmetry ansatz we find

$$m = \left[t_s \mathrm{erf}\left(\frac{m t_s}{\sqrt{2}R} \right) \right]_s, \tag{60}$$

$$R = \sqrt{\alpha} + 2\left[\phi\left(\frac{m t_s}{\sqrt{2}R} \right) \right]_s, \tag{61}$$

$$t_s \equiv \sum_{\mu}^{s} \rho_\mu / \sqrt{s}, \tag{62}$$

where ϕ is given by Eq. (10) and the averages $[\cdots]_s$ are

over the probability distribution $p(t_s)$ for having t_s when the distribution for n_μ is the trimodal of Eq. (12). Considering, for simplicity, the case $s = 2$, where $p(0) = u^2 + b^2/2$, $p(1) = bu = p(-1)$, and $p(2) = b^2/4 = p(-2)$, one finds

$$m = \frac{\sqrt{2}}{a}\left\{\frac{b}{2}\mathrm{erf}(m\sqrt{2}/R) + u\,\mathrm{erf}\left(\frac{m}{\sqrt{2}R}\right)\right\}, \tag{63}$$

$$R = \sqrt{\alpha} + \{b^2\phi(2m/R) + 4bu\phi(m/R) + (b^2 + 2u^2)/\sqrt{2\pi}\}. \tag{64}$$

When these equations are used in the free energy, Eq. (43) at $T = 0$, the phase diagram of Fig. 4 is obtained in which S2 is the region where the symmetric solution of two finite components is globally stable. The phase of globally stable mixed states is also shown there for comparison. The symmetric two-component state is thus stable over a very small part of the phase diagram. This is consistent with results for the Hopfield model (the case u=0) where the critical α for this solution is $\alpha_c^{(2)} \sim 0$.[24] It is also known that the critical α for the appearance of the *locally* stable solution of three finite symmetric components is $\alpha_c^{(3)} \sim 0.029$, in this model, and the dotted line in Fig. 2 gives the result of our calculations, which go along similar lines to the derivation of Eq. (62), for $u \geq 0$.

Two comments are now in order about the phase diagrams. First is that both of them follow from the replica symmetry ansatz, Eq. (45), which is not expected to be correct at very low temperature, particularly in regions where there is a sign of strong SG behavior, as is the case when the replica-symmetric states are globally stable. Allowance for replica-symmetry breaking will change somewhat the upper transition line, leading to mixed behavior at $T = 0$. It is beyond the scope of this paper to determine this change.

The same limitation applies to the lower parts of the boundaries in Fig. 3. Second, even within the replica-symmetry ansatz, the determination of these parts of the curves is not accurate enough to exhibit possible reentrant behavior as one expects to have when $b = 1$.[25] Nevertheless, the phase diagrams that are obtained should exhibit the main features of the model with a trimodal distribution.

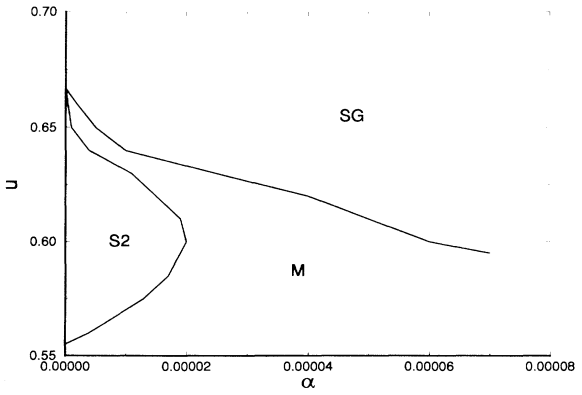

FIG. 4. Zero-temperature diagram showing the region S2 of global stability of the symmetric solution with two finite components.

V. DISCUSSION

In this paper we extended earlier works on the IRAM in two main aspects within mean-field theory. We considered (i) the large-component limit $p \to \infty$ and allowed for both $\alpha = 0$ and $\alpha \neq 0$, and (ii) we studied the effects of a trimodal probability distribution for the random axes with a finite probability that each component be either zero or finite.

In the $\alpha = 0$ case our work may be compared with that of FZ.[17] Their results are justified even in the limit $p \to \infty$, as long as $\alpha = 0$. We find stable ferromagnetic Mattis states, with a single finite component of the magnetization, that have lower free energy than other (mixed) states within a finite region of the (u, T) plane, where u is the probability for having a zero random-axis component. This is in contrast to the behavior found by FZ,[17] in which the limiting free energy per site becomes our Eqs. (16), with a cubic anisotropy, which is the lowest free energy when the number of nonzero magnetization components $s = p$. The stability of the symmetric magnetization found for $s = p$ is lost in our case where $p \to \infty$, if b is not very small. This behavior is due to the use of a noncubic random-axis distribution. Indeed, the cubic distribution for n_i^μ used in Ref. 17 favors a diagonal ordering already for finite p, in which each component of $O(1/\sqrt{p})$ becomes vanishingly small in the large-p limit.

Furthermore, in addition to F states, we have phases of mixed ordering and with residual order, when $\alpha = 0$, where the latter has a nonzero spin-glass order parameter, although there is no genuine spin-glass phase as long as $\alpha = 0$.

In the case where $\alpha \neq 0$, we find rather different behavior in that a mixed phase appears, in place of the diagonally ordered F phase of Ref. 17, referred to above. This phase competes for stability with a true spin-glass phase, and one or the other is more stable depending on the value of α, as discussed in detail in Sec. IV.

Unconstrained probability distributions for the random-axis vectors have often been used in the literature. Although easy to handle, a Gaussian distribution is not appropriate within MFT since it shares some of the problems of an isotropic distribution for fixed-length random vectors, in which a particular magnetization state is continuously degenerate. We have introduced here a trimodal distribution of statistically independent and identically distributed random-vector components. Depending on the size of b, Eq. (12), these components may deviate more or less from diagonal directions, enabling us thereby to study the effects of a varying anisotropy. All our results, for both $\alpha = 0$, or $\alpha \neq 0$, show a clear reduction of the size of the ordered regions in the phase

diagrams with departure from diagonal ordering.

Our work in MFT yields results independent of the dimensionality of the system. In order to determine the role of the latter, one would have to study the effect of fluctuations, which is beyond the scope of this work. Nevertheless, we believe that the general features of the phase diagrams should remain unchanged.

ACKNOWLEDGMENTS

This work was supported, in part, by Conselho Nacional de Desenvolvimento Científico e Tecnológico (CNPq), Financiadora de Estudos e Projetos (FINEP), and Fundação de Amparo à Pesquisa do Estado do Rio Grande do Sul (FAPERGS), Brazil.

[1] R. B. Harris, M. Plischke, and M. J. Zuckermann, Phys. Rev. Lett. **31**, 160 (1973). See also R. W. Cochrane, R. Harris, M. Plischke, D. Zobin, and M. J. Zuckermann, J. Phys. F **5** , 763 (1975).

[2] D. Mukamel and G. Grinstein, Phys. Rev. B **25**, 381 (1982); E. M. Chudnovsky, J. Appl. Phys. **64**, 5770 (1989).

[3] S. F. Edwards and P. W. Anderson, J. Phys. F **5**, 1965 (1975).

[4] See, for instance, S. G. Cornelison and D. J. Sellmyer, Phys. Rev. B **30**, 2845 (1984); D. J. Sellmyer and J. O'Shea, J. Less-Common Met. **94**, 59 (1984); D. J. Sellmyer and S. Nafis, J. Appl. Phys. **57**, 3584 (1985); R. Dieny and B. Barbara, J. Phys. (Paris) **46**, 293 (1985); Physica **130B**, 245 (1985); J. Tejada, B. Martinez, A. Labarta, R. Grossinger, H. Sassik, M. Vasquez, and A. Hernando, Phys. Rev. B **42**, 898 (1990).

[5] A. Aharony, Phys. Rev. B **12**, 1038 (1975).

[6] R. A. Pelcovits, E. Pytte, and J. Rudnick, Phys. Rev. Lett. **40**, 476 (1978); **48**, 1297(E) (1982).

[7] J. H. Chen and T. C. Lubensky, Phys. Rev. B **16**, 2106 (1977).

[8] A. Bray and M. Moore, J. Phys C **18**, L139 (1985).

[9] Y. Goldschmidt, Nucl. Phys. **B225** [FS9], 123 (1983). See also S. L. Ginsburg, Zh. Eksp. Teor **80**, 244 (1981) [Sov. Phys. JETP **53**, 124 (1981)]; **81**, 1389 (1981) [**54**, 737 (1981)].

[10] A. B. Harris, R. G. Caflisch, and J. R. Banavar, Phys. Rev. B **35**, 4929 (1987).

[11] R. Fisch and A. B. Harris, Phys. Rev. B **41**, 11305 (1990); J. Appl. Phys. **67**, 5778 (1990).

[12] A. Chakrabarti, Phys. Rev. B **36**, 5747(1987); J. Appl. Phys. **63**, 3735 (1988).

[13] R. Fisch, Phys. Rev. B **39**, 873 (1989).

[14] R. Fisch, Phys. Rev. B **39**, 873 (1989).

[15] C. Jayaprakash and S. Kirkpatrick, Phys. Rev. B **21**, 4072 (1980).

[16] B. Derrida and J. Vannimenus, J. Phys. C **13**, 3261 (1980).

[17] K. H. Fischer and A. Zippelius, J. Phys C **18**, L1139 (1985); Prog. Theor. Phys. Suppl. **87**, 165 (1986).

[18] J. J. Hopfield, Proc. Natl. Acad. Sci. USA **79**, 2554 (1982).

[19] D. J. Amit, *Modeling Brain Function* (Cambridge University Press, Cambridge, England, 1989).

[20] D. J. Amit, H. Gutfreund, and H. Sompolinsky, Phys. Rev. A **32**, 1007 (1985).

[21] D. J. Amit, H. Gutfreund, and H. Sompolinsky, Ann. Phys. (N.Y.) **173**, 30 (1987).

[22] A. E. Patrick and V. A. Zagrebnov, J. Stat. Phys. **63**, 59 (1991).

[23] D. Sherrington and S. Kirkpatrick, Phys. Rev. Lett. **35**, 1792 (1975).

[24] D. J. Amit, H. Gutfreund, and H. Sompolinsky, Phys. Rev. A **35**, 2293 (1987).

[25] J. P. Naef and A. Canning, J. Phys. (Paris) I **2**, 147 (1992).